

## Distribution and activity of Bacteria and Archaea in the deep water masses of the North Atlantic

*Eva Teira*<sup>1</sup>

Department of Biological Oceanography, Royal Netherlands Institute for Sea Research (NIOZ), P.O. Box 59, 1790 AB Den Burg, The Netherlands

*Philippe Lebaron*

Observatoire Océanologique, Laboratoire d'Océanologie Biologique de Banyuls, Université Paris VI, CNRS UMR 7621, BP44, F-66651 Banyuls-sur-Mer, France

*Hendrik van Aken*

Department of Physical Oceanography, Royal Netherlands Institute for Sea Research (NIOZ), P.O. Box 59, 1790 AB Den Burg, The Netherlands

*Gerhard J. Herndl*

Department of Biological Oceanography, Royal Netherlands Institute for Sea Research (NIOZ), P.O. Box 59, 1790 AB Den Burg, The Netherlands

### Abstract

We determined the distribution and activity of the major prokaryotic groups (Bacteria, *Cren-*, and *Euryarchaeota*) inhabiting the deep water masses of the North Atlantic by following the path of the North Atlantic Deep Water (NADW) from its formation in the Greenland-Iceland-Norwegian (GIN) Sea along its two major branches covering approximately the first 50 yr of the NADW in the oceanic conveyor belt system. The relative abundance of *Eury-* and *Crenarchaeota*, assessed by catalyzed reporter deposition-fluorescence in situ hybridization (CARD-FISH), was significantly higher in the western branch (17% and 24% of 4',6'-diamidino-2-phenylindole (DAPI)-stained cells, respectively) than in the eastern (9% and 17%, respectively) branch of the NADW. In contrast, the relative abundance of Bacteria (30% of DAPI-stained cells) did not differ between the western and the eastern basin. Prokaryotic production and turnover rates, however, were higher in the western than the eastern basin. Generally, the contribution of *Euryarchaeota* to total picoplankton was correlated positively with oxygen concentrations ( $p < 0.001$ ) and negatively with salinity ( $p < 0.001$ ) and temperature ( $p < 0.001$ ). The contribution of *Crenarchaeota* to total picoplankton correlated positively with oxygen ( $p < 0.05$ ) and negatively with salinity ( $p < 0.001$ ). There was a positive correlation between the crenarchaeotal contribution to picoplankton and nitrite concentration ( $p < 0.001$ ), especially in the oxygen minimum layer, suggesting their potential involvement in the marine nitrogen cycle as nitrifiers. The observed variability in archaeal abundance in relation to bulk prokaryotic activity supports the emerging notion that Archaea are a highly dynamic and metabolically active component of the deep ocean prokaryotic community.

The meso- and bathypelagic realm of the ocean makes up more than 70% of the global ocean's volume. It is commonly accepted that microbial biomass and activity are extremely low in the dark ocean and depend on the 30% of the organic matter, on average, exported from the euphotic

layer into the mesopelagic realm (Nagata et al. 2000). Direct measurements indicate one to two orders of magnitude decrease in bacterial abundance and production from the euphotic layer to the bathypelagic waters (Patching and Eardly 1997; Nagata et al. 2000; Hansell and Ducklow 2003).

The distribution of planktonic prokaryotes in a given oceanic habitat appears to be determined by local environmental conditions and not by restricted dispersal (Pedrós-Alió 1993; Finlay 2002). With the exceptions of the Mediterranean and the Sulu Sea, the global dark ocean exhibits a temperature range of 0–6°C and a salinity range between 34.6 and 37.8. The lack of geographic barriers for dispersion and the homogeneity of environmental conditions in the deep ocean may suggest a cosmopolitan distribution of most of the microbial inhabitants. Over the past few years, several studies on the distribution of the main prokaryotic groups have led to the conclusion that bacterial abundance decreases with depth, *Crenarchaeota*

<sup>1</sup>To whom correspondence should be addressed. Present address: Departamento Ecología e Biología Animal, Universidade de Vigo, Vigo, Spain (teira@uvigo.es).

### Acknowledgments

We thank the captain and crew of the R/V *Pelagia* for their help during work at sea, Karel Baker for inorganic nutrient analyses, and Philippe Catala for flow cytometry work.

This research was supported by a Marie Curie Fellowship of the European Community (HPMF-CT-2002-01738) to E.T., by a grant of the Earth and Life Science Division of the Dutch Science Foundation (NWO-ALW; project 811.33.004) to G.J.H., and by the 5th Framework Program of the Commission of the European Union (BASICS project).

are ubiquitously distributed and relatively more abundant in deep than in surface waters, while *Euryarchaeota* are relatively more prominent in surface than in deep waters (Massana et al. 2000; Karner et al. 2001; Church et al. 2003).

In contrast to this general vertical distribution pattern of the main prokaryotic groups, the functioning of the global ocean is primarily explained by the lateral transport of physically distinct water masses (thermohaline circulation) (Broecker 1997). Several recent studies have pointed to differences in the biogeographical distribution of the major groups of planktonic Archaea (López-García et al. 2001; Bano et al. 2004; Teira et al. 2006) and Bacteria (Giovannoni and Rappé 2000), which suggest that distinct water masses may harbor distinct prokaryotic communities.

The vertical distribution of prokaryotic plankton, where Bacteria dominates the upper water column and Archaea dominates the deep waters, suggests different resource utilization by the two main prokaryotic groups. Generally, more labile organic material is restricted to the upper ocean, and organic phosphorus and nitrogen are preferentially utilized by Bacteria, leading to an increase in the C:N:P ratio of dissolved organic matter (DOM) with depth (Bauer et al. 1992; Benner et al. 1992). Although our knowledge on the metabolic capabilities of planktonic Archaea is still rather limited, a few recent studies have shown that they are able to take up amino acids (Ouverney and Fuhrman 2000; Teira et al. 2004, 2006) but also inorganic carbon (Wuchter et al. 2003; Herndl et al. 2005). Recently, it has been shown that in meso- and bathypelagic waters of the North Atlantic, Bacteria preferentially utilize L-aspartic acid (Asp) over D-Asp, whereas *Crenarchaeota* do not discriminate between L- and D-forms of Asp (Teira et al. 2006). Thus, *Crenarchaeota* are mainly responsible for the observed increase in the bulk D:L-Asp uptake ratio with depth (Pérez et al. 2003; Teira et al. 2006).

Heretofore, only a few studies have related the distribution of the major prokaryotic groups to bulk (Massana et al. 1998; Murray et al. 1999) and group-specific prokaryotic activity in the deep ocean (Ouverney and Fuhrman 2000; Teira et al. 2004, 2006; Herndl et al. 2005). Clearly, more information is needed in order to identify the prokaryotes responsible for specific biochemical processes in the dark ocean and to determine whether the major water masses driving the oceanic conveyor belt circulation harbor specific prokaryotic communities.

In the present study, we determined the distribution of the three major prokaryotic groups (Bacteria, *Euryarchaeota*, and *Crenarchaeota*) in the main deep water masses of the North Atlantic. For this, we followed the North Atlantic Deep Water (NADW) from its formation in the Greenland-Iceland-Norwegian (GIN) Sea along two transects following the eastern and western branch of the NADW, covering approximately the first 50 yr of the NADW in the oceanic conveyor belt system. The main objective was to relate prokaryotic community composition to prokaryotic activity as determined by L-leucine and D- and L-Asp uptake by the bulk prokaryotic community.

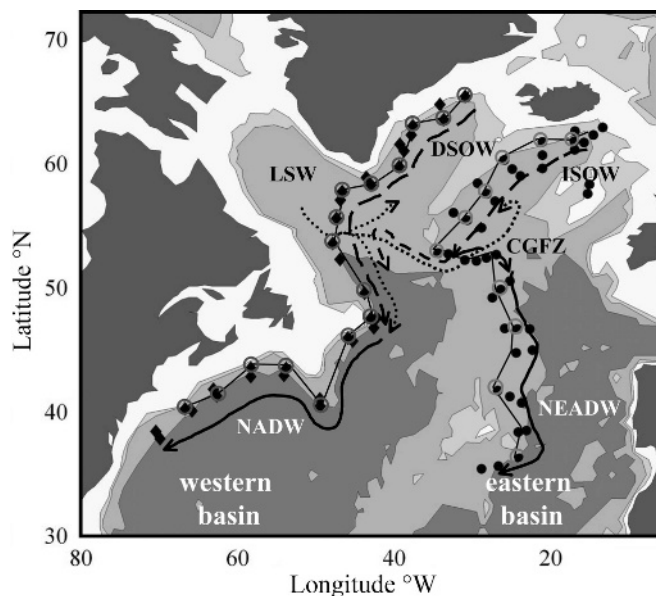


Fig. 1. Map of the cruise tracks (solid lines) and the flow of the main water masses (lines with arrows pointing to the flow direction). Sampling stations are indicated by closed circles for TRANSAT-1 (eastern basin) and by diamonds for TRANSAT-2 (western basin). Open circles indicate stations where CARD-FISH data on Bacteria and Archaea were collected. CGFZ, Charlie Gibbs Fracture Zone. For mass waters abbreviations, see the "sampling area" section.

## Material and methods

**Sampling area**—The eastern and western branches of the North Atlantic Deep Water (NADW) were followed during two cruises on board R/V *Pelagia* from the GIN Sea over >4000-km-long transects. TRANSAT-I (September 2002) followed a track from 62.8°N, 13.1°W to 35.3°N, 28.6°W in the eastern basin, and TRANSAT-II (May 2003), from 62.5°N, 30.3°W to 37.7°N, 69.7°W in the western basin of the North Atlantic (Fig. 1). In total, 42 and 36 stations were occupied during TRANSAT-I and TRANSAT-II, respectively. Water samples were collected with a CTD (conductivity, temperature, depth) rosette sampler holding 24 12-L NOEX bottles. Samples were taken from the 100–150-m layer (hereafter termed subsurface layer, SSL) at all the stations and, if present, from the oxygen minimum layer (O<sub>2</sub>-min), the Labrador Sea Water (LSW), the Iceland Scotland Overflow Water (ISOW), the North Atlantic Deep Water (NADW), the North East Atlantic Deep Water (NEADW), and the Denmark Strait Overflow Water (DSOW). Water masses were identified based on their salinity-temperature characteristics (Aken 2000a,b), and their oxygen concentrations were measured using a Seabird SBE43 oxygen sensor mounted on the CTD frame. Although prokaryotic abundance and production were measured at all the stations, the abundance of Bacteria, *Eury-*, and *Crenarchaeota* using fluorescence in situ hybridization (FISH) was only determined at selected stations (encircled stations in Fig. 1).

**Dissolved inorganic nutrients**—The concentrations of inorganic nutrients ( $\text{NH}_4^+$ ,  $\text{NO}_3^-$ ,  $\text{NO}_2^-$ ,  $\text{PO}_4^{3-}$ ,  $\text{SiO}_4^-$ ) were determined immediately after collecting the samples and gentle filtration through 0.2- $\mu\text{m}$  filters (Acrodisc, Gelman Science) in a TRAACS autoanalyzer system.  $\text{NH}_4^+$  was detected with the indo-phenol blue method (pH 10.5) at 630 nm (Helder and de Vries 1979).  $\text{NO}_2^-$  was determined after diazotization with sulfanilamide and *N*-(1-naphthyl)-ethylene diammonium-dichloride as the reddish-purple dye complex at 540 nm (Parsons et al. 1984).  $\text{NO}_3^-$  was reduced in a copper cadmium coil to nitrite (with imidazole as a buffer) and then measured as nitrite.  $\text{PO}_4^{3-}$  was determined via the molybdenum blue complex at 880 nm according to Murphy and Riley (1962).

**Prokaryotic abundance**—One milliliter seawater samples were fixed with 37% of 0.2- $\mu\text{m}$  filtered (Acrodisc, Gelman) formaldehyde (2% final conc.), stained with 0.5  $\mu\text{L}$  of SYBRGreen I (Molecular probes) at room temperature in the dark for 15 min, and subsequently analyzed on a FACSCalibur flow cytometer (BD Biosciences) (Lebaron et al. 1998). Counts were performed with the argon laser at 488 nm wavelength set at an energy output of 15 mW. Prokaryotic cells were enumerated according to their right-angle light scatter and green fluorescence measured at 530 nm.

**Prokaryotic production**—Bulk prokaryotic activity was measured by incubating 10–40 mL of water in duplicate and one formaldehyde-killed blank with 10 nmol  $\text{L}^{-1}$  [ $^3\text{H}$ ]-leucine (final conc., SA 5,957 and 5,587 GBq  $\text{mmol}^{-1}$  in TRANSAT-I and TRANSAT-II, respectively, Amersham) in the dark at in situ ( $\pm 1^\circ\text{C}$ ) temperature for 4–7 h, depending on the expected activity. Thereafter, the incubation was terminated by adding formaldehyde (2% final conc.) to the samples and filtering them through 0.2- $\mu\text{m}$  cellulose nitrate filters (Millipore, 25-mm filter diameter). Subsequently, the filters were rinsed three times with 5% ice-cold trichloroacetic acid, placed in scintillation vials, and stored at  $-20^\circ\text{C}$  until counting in a liquid scintillation counter. The disintegrations per minute (DPM) of the formaldehyde-fixed blank were subtracted from the samples, and the resulting DPM was converted into leucine incorporation rates (Herndl et al. 2005; Reinthaler et al. in press).

**Uptake of D- and L-Asp by the bulk prokaryotic community**—To measure the uptake of D- and L-Asp by the bulk prokaryotic community, 20–40 mL of duplicate water samples and one formaldehyde-killed blank (2% final conc.) were spiked with either D-[2,3- $^3\text{H}$ ]-Asp or L-[2,3- $^3\text{H}$ ]-Asp (Amersham, SA: D-Asp, 481 GBq  $\text{mmol}^{-1}$ ; L-Asp, 1,369 GBq  $\text{mmol}^{-1}$ ) at a final concentration of 1 nmol  $\text{L}^{-1}$  and incubated in the dark at in situ temperature for 4–7 h. After terminating the incubations by adding formaldehyde (2% final conc.), the samples were filtered through 0.2- $\mu\text{m}$  cellulose nitrate filters (Millipore, 25-mm filter diameter), rinsed twice with 0.2- $\mu\text{m}$ -filtered seawater, and stored in scintillation vials at  $-20^\circ\text{C}$  until analysis. Back in the laboratory, filters were dissolved in 1-

mL ethyl acetate (Riedel de Haen), and, after 10 min, 8 mL of scintillation cocktail (Insta-gel plus II, Canberra Packard) was added. After 18 h, the radioactivity of the filters was assessed in a liquid scintillation counter by counting each sample for 10 min. The DPM of the formaldehyde-fixed blank were subtracted from the corresponding samples, and the resulting DPM was converted into D- and L-Asp uptake rates. The mean coefficient of variation between replicates was  $10 \pm 9\%$  and  $8 \pm 9\%$  for the D- and L-Asp uptake rate, respectively, and the DPM of the blanks were always  $<40\%$  of the mean DPM of the respective duplicate samples. A final concentration of 1 nmol  $\text{L}^{-1}$  of radiolabeled Asp was used for bulk D- and L-Asp uptake measurements since the concentration of dissolved free Asp in the North Atlantic Deep Water is  $<5$  nmol  $\text{L}^{-1}$ , and Pérez et al. (2003) showed that uptake rates increase from 0.1 nmol  $\text{L}^{-1}$  to 10 nmol  $\text{L}^{-1}$  final concentration of added Asp by a factor of  $\sim 10$ .

**Catalyzed reporter deposition-FISH (CARD-FISH)**—Immediately after collecting the samples from the NOEX bottles, water samples of 20–40 mL were fixed by adding 0.2- $\mu\text{m}$  filtered paraformaldehyde (2% final conc.), and, subsequently, the samples were stored at  $4^\circ\text{C}$  in the dark for 12–18 h. Thereafter, the sample was filtered through a 0.2- $\mu\text{m}$  polycarbonate filter (Millipore, GTTP, 25-mm filter diameter) supported by a cellulose nitrate filter (Millipore, HAWP, 0.45  $\mu\text{m}$ ), washed twice with Milli-Q water, and dried and stored in a microfuge vial at  $-20^\circ\text{C}$  until further processing in the home laboratory.

Filters for CARD-FISH were embedded in low-gelling-point agarose and incubated either with lysozyme (for the Bacteria probe Eub338 and for the negative control probe Non338; Amann et al. 1995) or proteinase-K (for the *Euryarchaeota* probe Eury806 [5'-CACAGCGTTTACACCTAG-3'] and for the *Crenarchaeota* probe Cren537 [5'-TGACCACTTGAGGTGCTG-3']; Teira et al. 2004). Filters were cut in sections and hybridized with horseradish peroxidase (HRP)-labeled oligonucleotide probes and tyramide-Alexa488 for signal amplification following the protocol described in Teira et al. (2004). Cells were counterstained with a DAPI-mix (5.5 parts of Citifluor [Citifluor, Ltd.], 1 part of Vectashield [Vector Laboratories, Inc.] and 0.5 parts of phosphate-buffered saline (PBS) with DAPI [final concentration 1  $\mu\text{g mL}^{-1}$ ]).

The slides were examined under a Zeiss Axioplan 2 microscope equipped with a 100-W Hg lamp and appropriate filter sets for DAPI and Alexa488. More than 800 DAPI-stained cells were counted per sample. For each microscope field, two different categories were enumerated: (1) total DAPI-stained cells, (2) cells stained with the specific probe. Negative control counts (hybridization with HRP-Non338) averaged 1.5% and were always below 5% of DAPI-stained cells. The counting error, expressed as the percentage of standard error between replicates, was  $<2\%$  for DAPI counts and  $<9\%$  for FISH counts.

**Statistical analysis**—Logarithmic transformation was conducted for linear regression analysis. ANCOVA *F*-test was used for slope comparison of two regression lines. For

correlation analysis, the Spearman coefficient was used instead of Pearson because some variables did not comply with normality even after logarithmic transformation. The non-parametric Mann-Whitney test was used for mean comparison of two independent samples if normality was not attained, and the *t*-test was used if data followed normal distribution.

## Results

**Water mass characteristics**—The flow of the main water masses is indicated in Figure 1, and the basic physical-chemical characteristics of these main water masses sampled during this study are summarized in Table 1. The distribution of temperature, salinity, and oxygen concentration along the transect in the eastern and western basin of the North Atlantic is shown in Figure 2, the distribution of inorganic nutrients (nitrate, phosphate, and silicate), in Figure 3.

The Iceland Scotland Overflow Water (ISOW), which originates from the Nordic seas (McCartney et al. 1998), flows to the south in the eastern basin and was detected close to the bottom from 62°N to 52°N. The Labrador Sea Water (LSW), characterized by low salinity, was clearly identifiable at depth levels between 800 and 2,100 m throughout the western transect, except between 40°N and 45°N. In the eastern basin, the LSW was identifiable at deeper depth horizons (1,600–2,000 m), but the core water (salinity < 34.9) was found around the latitude of the Charlie Gibbs Fracture Zone, through which the LSW enters the eastern basin of the North Atlantic (Rhein et al. 2002). The NEADW (2,300–3,000 m), characterized by a salinity maximum (>34.92), is formed in the eastern basin south of the Charlie Gibbs Fracture Zone (Aken 2000*a,b*). The influence of the outflow of water from the Mediterranean Sea increases the NEADW salinity signal at the southern end of the transect (>34.95) (Aken 2000*a,b*). The NADW (2,400–2,800 m) of the western basin (Smethie et al. 2000) was identifiable by its salinity maximum (34.9–34.95) south of 60°N. The DSOW underlying the NADW, with a seawater temperature between 0.8 and 2.4°C and salinity <34.9 (Table 1), was detected at all the stations between 45°N and 65°N. A local oxygen minimum (<250 μmol L<sup>-1</sup>) was found between 200 m and 600 m depth in the southern part of the western basin (from 40°N to ~50°N) (Fig. 2). In the eastern basin, the oxygen minimum (O<sub>2</sub>-min) zone was found throughout the transect and was located at greater depths than in the western basin. The maximum oxygen concentration in the O<sub>2</sub>-min was lower in the eastern than in the western basin (Table 1).

As ISOW/NEADW flows southwards in the eastern basin, the salinity and oxygen concentrations decrease, and the concentrations of dissolved inorganic nutrients (Fig. 3) increase, partially due to mixing with over- and underlying water masses and partly due to remineralization processes (Hansell 2002).

Temperature, salinity, and inorganic nutrient concentrations (nitrate, phosphate, and silicate) were significantly higher in the eastern than in the western basin (Table 1; Mann-Whitney test, *p* < 0.02, *n* = 140), whereas ammonia,

nitrite, and oxygen concentrations were significantly lower in the eastern than in the western basin (Table 1; Mann-Whitney test, *p* < 0.001, *n* = 140).

**Prokaryotic abundance and activity**—Prokaryotic abundance decreased exponentially with depth (Reinthal et al. in press); however, the different deep water masses exhibited pronounced differences in prokaryotic abundance, and latitudinal trends were apparent (Fig. 4). The SSL in the western basin generally exhibited a higher prokaryotic abundance than in the eastern basin. This was probably also due to the greater mean sampling depth in the eastern basin (138 m) than in the western basin (100 m). The ISOW and DSOW originating north of 60°N harbored a higher prokaryotic abundance than the subsequently formed NEADW and NADW. In the northeastern basin, the ISOW is in direct contact with the seafloor. Thus, it carries relatively high concentrations of resuspended sediment and prokaryotes (Reinthal et al. in press). Consequently, prokaryotic abundance in the ISOW was higher than in the overlying LSW (Fig. 4).

Despite the higher prokaryotic abundance in the SSL of the western than the eastern basin, the mean prokaryotic abundance in the deep water masses was higher in the eastern than in the western basin (*t*-test, *p* < 0.001, *n* = 137).

Leucine incorporation, as a measure of prokaryotic activity, followed a similar pattern as that of abundance, decreasing with depth by one order of magnitude (Table 2; Fig. 4). However, prokaryotic activity was significantly higher in the western than in the eastern basin (*t*-test, *p* < 0.01, *n* = 136; Fig. 5). As for abundance, prokaryotic activity in the ISOW was higher than in the overlying LSW. In the LSW, prokaryotic activity in the western basin was approximately twice as high as in the eastern basin (Table 2; Fig. 5). Also in the O<sub>2</sub>-min layer and the NADW of the western basin, prokaryotic activity was higher than in the corresponding water masses of the eastern basin (Table 2).

The D:L-Asp uptake ratio of prokaryotes increased with depth in both the eastern and western basin (Table 2; Fig. 4). As for prokaryotic abundance and leucine incorporation, the D:L-Asp uptake ratio appeared to be more related, however, to the different water masses rather than to depth (Fig. 5). In the eastern basin, the D:L-Asp uptake ratio increased from the SSL to the LSW (Table 2; Fig. 5) but decreased again in the ISOW, close to the bottom. As ISOW flowed southwards and formed the NEADW by mixing with LSW and Lower Deep Water, the D:L-Asp uptake ratio increased again in the NEADW. The highest D:L-Asp uptake ratios (>2) were measured in the LSW and NEADW close to the Charlie Gibbs Fracture Zone (Fig. 4). In the western basin, the D:L-Asp uptake ratio increased with depth from the SSL to the NADW, but decreased again in the DSOW underlying the NADW (Fig. 5). No significant differences were found in the mean D:L-Asp uptake ratios between the eastern and western basin (*t*-test, *p* = 0.138, *n* = 124).

A negative log-log linear relationship was found between D:L-Asp uptake ratios and leucine incorporation for both

Table 1. Physical and chemical characteristics of the major water masses in the eastern and western basins of the North Atlantic. Mean and ranges (in parentheses) are given for each water mass where samples were collected. See the "sampling area" section for water mass abbreviations.

Basin	Water mass	Depth (m)	Temperature (°C)	Salinity	Oxygen ( $\mu\text{mol L}^{-1}$ )	Nitrate ( $\mu\text{mol L}^{-1}$ )	Nitrite ( $\mu\text{mol L}^{-1}$ )	Ammonia ( $\mu\text{mol L}^{-1}$ )	Phosphate ( $\mu\text{mol L}^{-1}$ )	Silicate ( $\mu\text{mol L}^{-1}$ )
Eastern	SSL	138	10.0	35.3	244	12.4	0.022	0.11	0.8	5.4
		(90–150)	(6.20–15.10)	(34.90–36.06)	(209–268)	(5.6–16.1)	(0.014–0.036)	(0.07–0.24)	(0.35–1.06)	(2.3–7.8)
	O <sub>2</sub> -min	672	6.6	35.1	215	19.3	0.012	0.11	1.3	10.9
		(400–1,000)	(4.98–10.37)	(34.90–35.54)	(183–233)	(17.8–20.3)	(0.004–0.023)	(0.05–0.24)	(1.11–1.34)	(7.6–11.5)
	LSW	1,798	3.4	34.91	270	17.7	0.008	0.10	1.2	12.0
	ISOW	(1,600–2,000)	(3.07–3.92)	(34.88–35.02)	(247–276)	(16.7–18.6)	(0.003–0.015)	(0.06–0.23)	(1.12–1.23)	(10.9–14.02)
2,314		2.6	34.97	273	16.1	0.016	0.14	1.3	12.3	
NEADW	(1,700–3,100)	(1.87–3.08)	(34.96–34.98)	(265–281)	(15.5–16.9)	(0.012–0.021)	(0.09–0.22)	(1.04–1.15)	(9.74–16.81)	
	2,759	3.0	34.95	257	18.2	0.008	0.10	1.2	19.5	
	(2,300–3,000)	(2.87–3.14)	(34.93–34.97)	(237–268)	(16.6–20.6)	(0.002–0.012)	(0.06–0.16)	(1.12–1.38)	(13.0–26.9)	
Western	SSL	100	8.3	35.1	269	12.0	0.16	0.20	0.8	6.4
		(90–110)	(4.10–18.80)	(34.56–36.60)	(206–305)	(1.9–16.1)	(0.039–0.295)	(0.10–0.40)	(0.09–1.09)	(0.9–8.2)
	O <sub>2</sub> -min	410	7.5	35.04	178	20.7	0.021	0.14	1.3	12.5
		(200–600)	(4.20–10.10)	(34.79–35.29)	(144–257)	(16.4–23.6)	(0.014–0.034)	(0.10–0.20)	(1.09–1.49)	(9.5–14.2)
	LSW	1,330	3.4	34.88	281	16.6	0.011	0.13	1.1	10.4
		(800–2,100)	(3.08–3.70)	(34.86–34.94)	(262–287)	(16.1–17.5)	(0.005–0.018)	(0.08–0.18)	(1.08–1.16)	(9.5–12.1)
NADW	2,558	2.9	34.92	273	16.8	0.011	0.13	1.1	14.9	
DSOW	(2,400–2,800)	(2.55–3.17)	(34.90–34.95)	(265–279)	(16.1–17.9)	(0.007–0.016)	(0.07–0.19)	(1.06–1.19)	(12.2–18.1)	
	2,916	1.9	34.88	290	15.0	0.013	0.13	1.0	13.5	
	(1,200–3,900)	(0.84–2.38)	(34.81–34.90)	(269–311)	(12.5–17.8)	(0.004–0.040)	(0.07–0.18)	(0.87–1.20)	(6.5–25.2)	

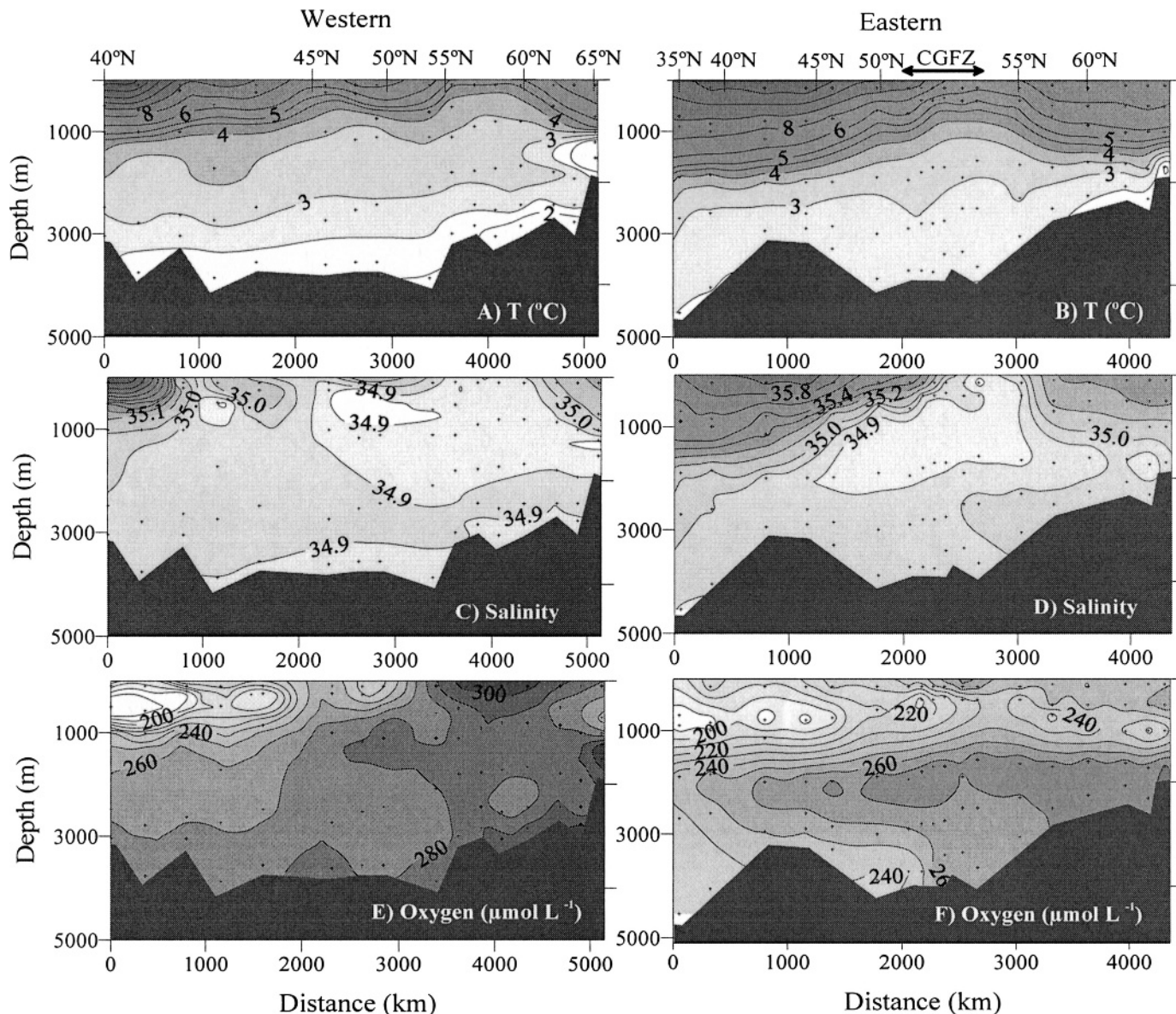


Fig. 2. Distribution of (A, B) temperature,  $T$ , (C, D) salinity, and (E, F) oxygen concentration along the western and eastern transect in the North Atlantic. Sampling locations are indicated by crosses. The location of the Charlie Gibbs Fracture Zone (CGFZ) is indicated on panel B.

the eastern and western basin (Fig. 6). As indicated in Figure 6, leucine uptake rates can explain only 10% and 30% of the observed variability in the D:L-Asp uptake ratios in the eastern and western basin, respectively. The slope of the regression for the western basin was significantly different from that for the eastern basin (ANCOVA  $F$  test,  $p < 0.0001$ ). The relatively high D:L-Asp uptake ratios obtained in the SSL of the eastern basin (0.23 versus 0.09 in the western basin; Table 2; Fig. 5) were likely responsible for the differences in the slope of the regression, probably reflecting the greater sampling depth of the SSL in the eastern (135 m) compared to the western basin (100 m).

*Prokaryotic community composition*—Bacterial, cren-, and euryarchaeotal abundance was determined by

CARD-FISH with HRP-oligonucleotide probes. For each sample, counts obtained with each of the specific probes were related to the abundance of DAPI-stainable cells referred to as picoplankton. The number of DAPI-stained cells before and after CARD-FISH processing was not significantly different (Teira et al. 2004), indicating that loss of cells during CARD-FISH processing was negligible. Prokaryotic abundance determined by flow cytometry was significantly higher than picoplankton abundance obtained by epifluorescence microscopy of DAPI-stained cells ( $t$ -test,  $p = 0.008$ ,  $n = 112$ ). However, there was a highly significant log-log linear relationship between the prokaryotic abundance determined by flow cytometry (FC) and picoplankton abundance determined by DAPI staining ( $\log \text{DAPI} = 0.86 \times \log \text{FC} - 0.226$ ,  $r^2 = 0.80$ ,  $p < 0.001$ ,  $n = 112$ ). The difference between both estimates was  $<14\%$ .

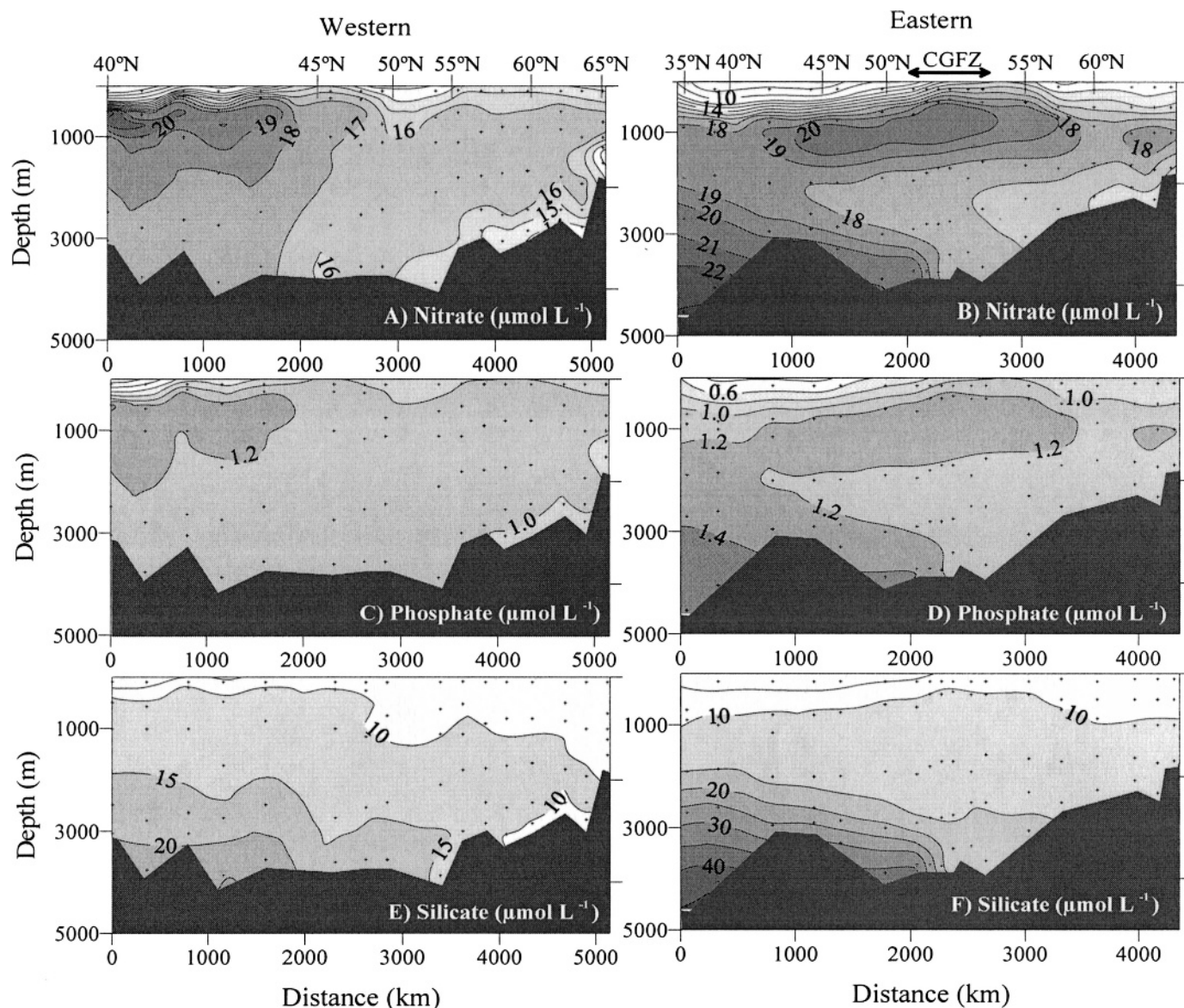


Fig. 3. Distribution of (A, B) nitrate, (C, D) phosphate and (E, F) silicate concentration along the western and eastern transect in the North Atlantic. Sampling locations are indicated by crosses. Location of the Charlie Gibbs Fracture Zone (CGFZ) is indicated on panel B.

The mean contributions of Bacteria, *Cren-*, and *Euryarchaeota* to total picoplankton abundance for the different water masses are given in Table 2. Bacteria contributed to total picoplankton abundance between 24% and 33%, and there was no significant difference between the eastern and western basin nor between water masses (Table 2).

The relative abundance of *Crenarchaeota* ranged from 9% in the NEADW to 27% in the NADW (Table 2). Overall, *Crenarchaeota* contributed significantly more (*t*-test,  $p < 0.001$ ,  $n = 114$ ) to the total picoplankton community in the western (17–27%) than in the eastern (9–23%) basin, and were most abundant in the oxygen minimum layer and in the NADW (Table 2).

The relative abundance of *Euryarchaeota* was also significantly higher (*t*-test,  $p < 0.01$ ,  $n = 113$ ) in the

western (16–18%) than in the eastern (7–11%) basin (Table 2). The percentage of picoplankton identified as *Euryarchaeota* was lowest in the ISOW (mean 7%), which is in striking contrast to the relatively high euryarchaeotal contribution of 24% detected in the DSW (Table 2).

Total CARD-FISH detectable cells, representing the sum of the relative abundance of Bacteria, *Cren-*, and *Euryarchaeota* averaged  $71 \pm 2\%$  ( $n = 72$ ) and  $57 \pm 2\%$  ( $n = 39$ ) of total DAPI-stainable cells in the western and eastern North Atlantic basins, respectively.

*Environmental factors and prokaryotic community structure and function*—The contribution of *Cren-* and *Euryarchaeota* to the prokaryotic community was closely related to the water masses sampled. The contribution of Bacteria to the prokaryotic community showed little

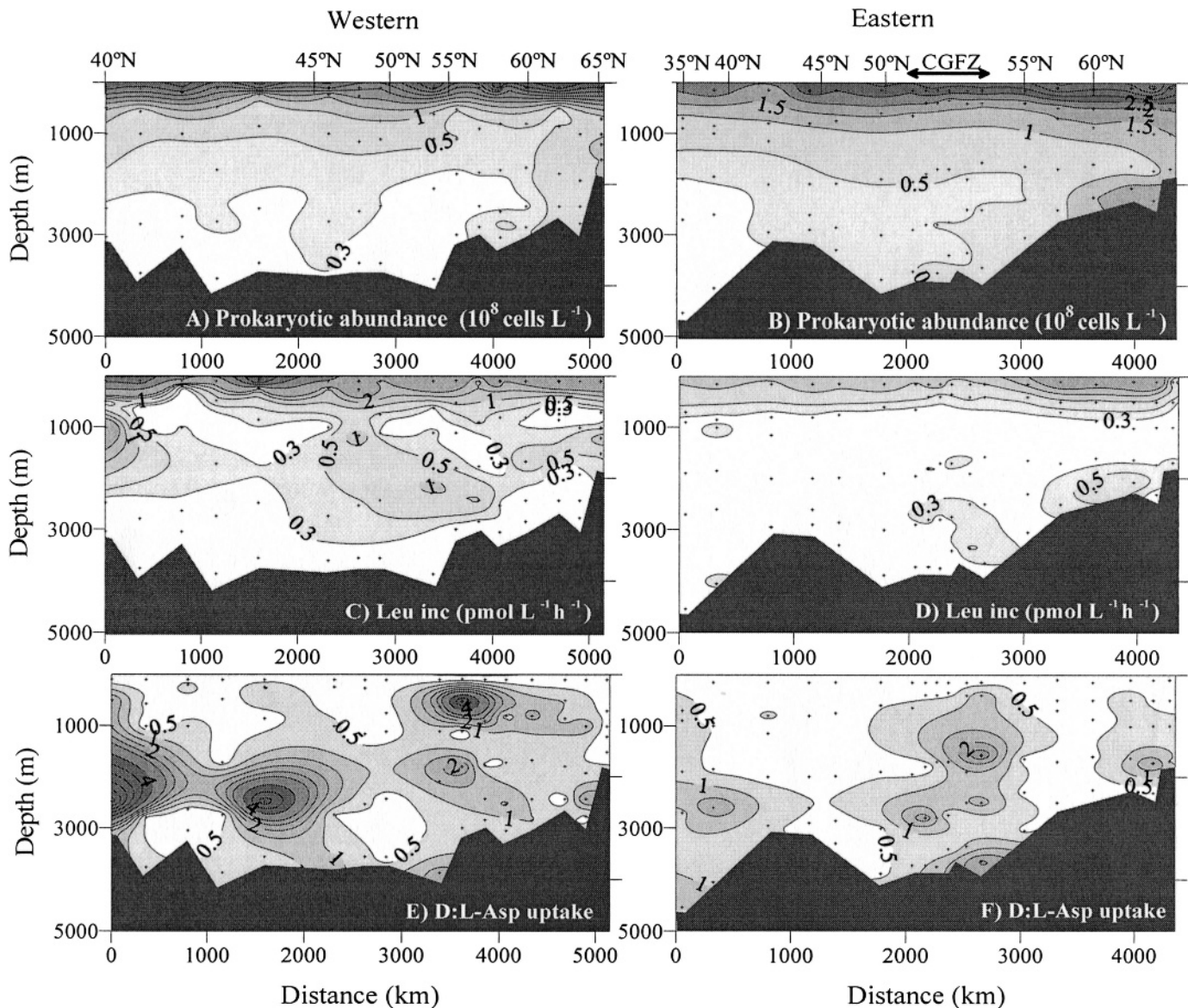


Fig. 4. Distribution of (A, B) prokaryotic abundance, (C, D) leucine incorporation, and (E, F) D:L-Aspartic acid uptake ratio along the western and eastern transect in the North Atlantic.

variability (in >70% of the samples, the contribution ranged between 25% and 40%), and no significant differences were found between water masses.

We analyzed the relation between the contribution of these three prokaryotic groups and the main environmental variables, such as temperature, salinity, oxygen, and dissolved inorganic nutrient concentrations in the meso- and bathypelagic waters of the North Atlantic (Table 3). Overall, the relative abundance of *Crenarchaeota* was negatively correlated to salinity and nitrate concentration and positively correlated to nitrite and oxygen. *Euryarchaeota* were positively correlated to oxygen concentration and negatively correlated to temperature, salinity, nitrate, and phosphate concentrations. Despite the significance of these correlations, each of the environmental factors could explain only between 5% and 17% of the observed variability in the distribution of *Cren-* and *Euryarchaeota*.

Bacterial contribution to total picoplankton abundance, however, did not show any correlation to any of the physical-chemical variables (Table 3). This lack of correlation is not surprising, since Bacteria represent a much more diverse group than *Eury-* and *Crenarchaeota*.

The corresponding relation between the contributions of the three prokaryotic groups and the main microbiological variables is shown in Table 4. *Euryarchaeota* were positively correlated to leucine incorporation, and, interestingly, only *Crenarchaeota* exhibited a positive correlation with D-Asp uptake.

While in the western basin, Archaea, i.e., the sum of *Cren-* and *Euryarchaeota*, clearly dominated the prokaryotic community, in the eastern basin, Archaea and Bacteria contributed roughly equally to the picoplankton community (Table 2). The D:L-Asp uptake ratio appeared to be more tightly linked to the relative abundance of Archaea,

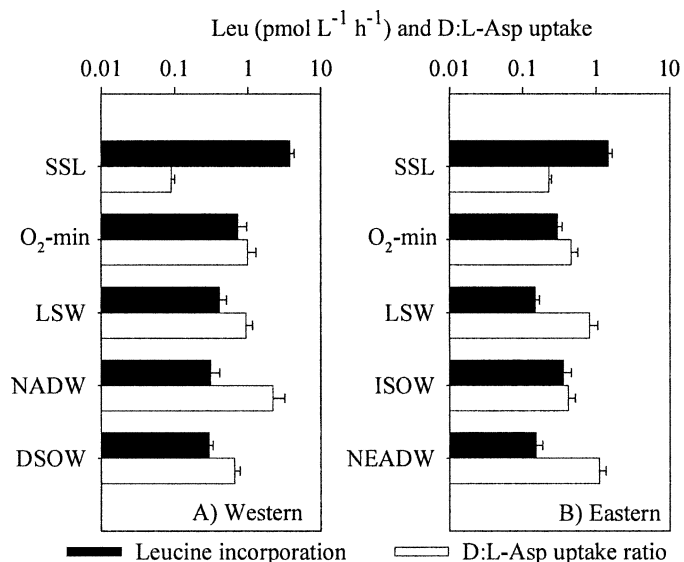


Fig. 5. Mean ( $\pm$ SE) of leucine uptake and D:L-Asp uptake ratio in the different water masses in (A) the western and (B) eastern basins of the North Atlantic.

and particularly to *Crenarchaeota*, than to leucine incorporation (compare Figs. 6 and 7). The higher the contribution of *Crenarchaeota* to the picoplankton abundance, the higher the D:L-Asp uptake ratio, with the remarkable exception of the NEADW (Fig. 7).

## Discussion

The NADW is formed by several water masses originating in both the eastern and western basins of the North Atlantic. Despite the importance of deep water circulation for the meridional ocean circulation and the global climate, our knowledge of microbiological processes in these cold, deep water masses is still in its infancy. From the data presented here, it is evident that the different deep water masses maintain specific microbiological properties during their lateral flow in the oceanic conveyor belt.

Table 2. Relative contribution of Bacteria (Bact), *Crenarchaeota* (Cren), and *Euryarchaeota* (Eury) to the total prokaryotic community expressed as % DAPI-stained cells and the uptake rates of leucine (Leu) and D- and L-aspartic acid (Asp) of the bulk prokaryotic community expressed in  $\text{pmol L}^{-1} \text{h}^{-1}$ . Mean  $\pm$ SE is given.

Basin	Water mass*	$n_1$	Bact	Cren	Eury	$n_2$	Leu	D-Asp	L-Asp	D:L-Asp
Eastern	SSL	9	29 $\pm$ 4	19 $\pm$ 3	10 $\pm$ 2	17	1.46 $\pm$ 0.19	1.01 $\pm$ 0.15	4.5 $\pm$ 0.7	0.23 $\pm$ 0.02
	O <sub>2</sub> -min	10	29 $\pm$ 2	19 $\pm$ 3	10 $\pm$ 3	17	0.30 $\pm$ 0.05	0.24 $\pm$ 0.04	0.76 $\pm$ 0.16	0.46 $\pm$ 0.11
	LSW	9	30 $\pm$ 3	21 $\pm$ 4	9 $\pm$ 2	14	0.15 $\pm$ 0.02	0.10 $\pm$ 0.02	0.17 $\pm$ 0.02	0.8 $\pm$ 0.2
	ISOW	5	30 $\pm$ 2	23 $\pm$ 2	7 $\pm$ 1	7	0.36 $\pm$ 0.10	0.23 $\pm$ 0.04	0.72 $\pm$ 0.19	0.42 $\pm$ 0.11
	NEADW	3	24 $\pm$ 1	9 $\pm$ 2	11 $\pm$ 3	13	0.15 $\pm$ 0.04	0.08 $\pm$ 0.02	0.11 $\pm$ 0.03	1.1 $\pm$ 0.03
Western	SSL	16	32 $\pm$ 2	17 $\pm$ 2	17 $\pm$ 2	16	3.8 $\pm$ 0.6	0.41 $\pm$ 0.06	4.6 $\pm$ 0.6	0.09 $\pm$ 0.01
	O <sub>2</sub> -min	7	33 $\pm$ 3	26 $\pm$ 3	16 $\pm$ 3	7	0.7 $\pm$ 0.2	0.28 $\pm$ 0.07	0.7 $\pm$ 0.3	1 $\pm$ 0.3
	LSW	14	30 $\pm$ 2	22 $\pm$ 2	17 $\pm$ 2	17	0.41 $\pm$ 0.10	0.15 $\pm$ 0.03	0.26 $\pm$ 0.06	0.9 $\pm$ 0.2
	NADW	11	32 $\pm$ 2	27 $\pm$ 2	18 $\pm$ 2	12	0.31 $\pm$ 0.10	0.08 $\pm$ 0.02	0.09 $\pm$ 0.02	2.2 $\pm$ 1
	DSOW	11	27 $\pm$ 2	24 $\pm$ 2	17 $\pm$ 2	12	0.29 $\pm$ 0.04	0.15 $\pm$ 0.02	0.6 $\pm$ 0.2	0.67 $\pm$ 0.12

\* See the "sampling area" section for water mass abbreviations;  $n_1$ , number of samples for prokaryotic community composition;  $n_2$ , number of samples for uptake rate measurements.

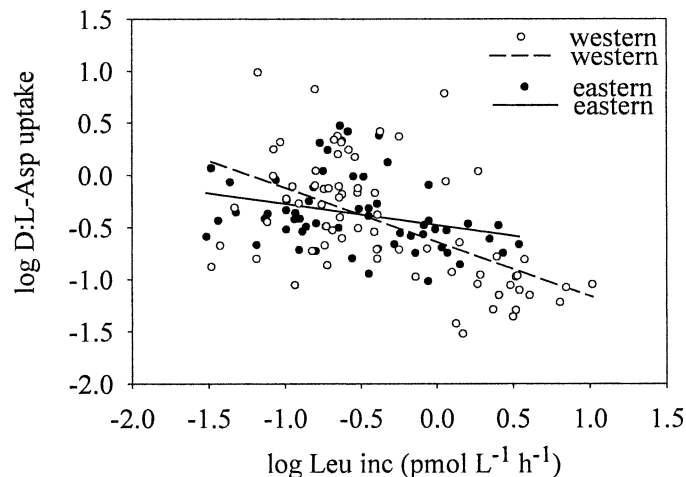


Fig. 6. Log-log relationship between leucine incorporation and D:L-Asp uptake ratio in the western and eastern basins of the North Atlantic. Regression line equations are:  $\log \text{D:L-Asp} = -0.21 \times \log \text{Leu} - 0.48$ ,  $r^2 = 0.10$ ,  $p = 0.02$ ,  $n = 60$ , for the eastern basin; and  $\log \text{D:L} = -0.52 \times \log \text{Leu} - 0.64$ ,  $r^2 = 0.30$ ,  $p < 0.001$ ,  $n = 72$ , for the western basin.

*Prokaryotic distribution in distinct water masses of the North Atlantic*—Despite the rather homogeneous environmental conditions predominating in the dark and cold deep ocean, we observed remarkable differences between the prokaryotic community structure in the eastern and western North Atlantic basins (Table 2).

The mean relative contribution of Bacteria to total picoplankton community did not significantly differ between the eastern and western basin of the North Atlantic and did not show any clear trend with depth nor with latitude (Table 2).

The percentage of DAPI-stained cells identified as Bacteria in the deep waters of the North Atlantic was considerably lower than in previous studies (Karner et al. 2001; Church et al. 2003). The mean values for the different water masses ranged from 24% to 33% (Table 2), whereas percentages between 30% and 70% were found for the same depth range in the Pacific (Karner et al. 2001) and the

Table 3. Spearman rank correlation of the relative abundance (% of DAPI-stained cells) of Bacteria (Bact), *Crenarchaeota* (Cren), and *Euryarchaeota* (Eury) with physicochemical variables in the deep waters of the North Atlantic.

$n = 84$	Temperature	Salinity	Oxygen	Nitrate	Nitrite	Ammonia	Phosphate	Silicate
Bact	0.110	0.070	-0.024	0.067	-0.149	0.089	0.029	0.016
Cren	-0.137	-0.324**	0.224*	-0.239*	0.285**	-0.057	-0.188	0.029
Eury	-0.307**	-0.416**	0.413**	-0.323**	0.194	-0.040	-0.282**	0.058

\*  $p < 0.05$ .

\*\*  $p < 0.001$ .

Southern Ocean (Church et al. 2003). The main difference between these studies and ours is the use of polynucleotide probes in the previous studies, whereas we used the oligonucleotide probe Eub338 (Teira et al. 2004) to detect and enumerate Bacteria. It has been shown that the use of this single probe is insufficient to detect all Bacteria because it does not target members of *Verrucomicrobia* and *Planctomycetales* (Daims et al. 1999). These authors designed two probes complementary to Eub338: Eub338-II and Eub338-III. To assess the potential bias introduced by using only the Eub338 probe, we compared the percentage of DAPI-stained cells labeled with the single Eub338 with that using a mix of Eub338/Eub338-II/Eub338-III in a total of 20 samples (4 stations  $\times$  5 depths) in the North Atlantic. The percentage of Bacteria was significantly higher when using the mix of Eub338 probes ( $t$ -test,  $p < 0.001$ ,  $n = 20$ ), and mean contributions of Bacteria to total DAPI-stained cells ranged between 30% and 50%. The differences were highest at 100- and 3500-m depth. Overall, we might have underestimated the actual contribution of Bacteria to total prokaryotic abundance by, on average,  $11 \pm 1\%$  (data not shown).

In contrast to Bacteria, both *Crenarchaeota* and *Euryarchaeota* contributed significantly more to the total picoplankton abundance in the western than the eastern basin (Table 2). These basin-scale differences in the distribution pattern of Archaea might be related to deep water mass formation processes. The most pronounced difference in euryarchaeotal contribution to total picoplankton was observed between the two coldest sources of the NADW, the ISOW and the DSOW. Whereas the relative contribution of Bacteria and *Crenarchaeota* was similar (Table 2) in both water masses, the contribution of *Euryarchaeota* was more than two times higher in the DSOW (17% of DAPI-stained cells) than in the ISOW (7% of DAPI-stained cells). Both water masses originate in the

Table 4. Spearman rank correlation of the relative abundance (% of DAPI-stained cells) of Bacteria (Bact), *Crenarchaeota* (Cren), and *Euryarchaeota* (Eury) with uptake rates of leucine (Leu), D- and L-aspartic acid (Asp), and the D:L-Asp uptake ratio in the deep waters of the North Atlantic.

$n = 84$	Leu	D-Asp	L-Asp	D:L-Asp
Bact	-0.014	-0.230*	-0.220*	0.071
Cren	0.196	0.215*	0.156	-0.131
Eury	0.276*	-0.160	-0.263*	0.209

\*  $p < 0.05$ .

Nordic and Polar Seas and subsequently flow over the Greenland-Iceland-Faroe-Scotland Ridge (McCartney et al. 1998). Despite their common origin, during the formation of ISOW, warmer overlying water is entrained into the turbulent bottom current near the Iceland-Faroe Ridge. By mixing with this warmer water, the temperature of the ISOW rises from  $\sim 0^\circ\text{C}$  to  $\sim 2^\circ\text{C}$ . This warmer overlying water was detected north of  $60^\circ\text{N}$  in the eastern transect (Fig. 2) where the water temperature was  $>5^\circ\text{C}$  down to  $\sim 1,400$  m. This warmer water mass was characterized by very low euryarchaeotal abundance ( $<5\%$  of DAPI-stained cells; data not shown). The increase in abundance of *Euryarchaeota* in the NEADW in the eastern basin further south might be related to the entrainment of LSW from the western basin through the Charlie Gibbs Fracture Zone. After the LSW passes the Charlie Gibbs Fracture Zone, it then flows south and north, mixing with adjacent water masses. Euryarchaeotal contribution to picoplankton in the LSW of the western basin is  $>16\%$  of DAPI-stained cells, while it is 9% of DAPI-stained cells in the eastern basin (Table 2). The negative correlation of euryarchaeotal abundance with temperature and salinity and the corresponding positive correlation with oxygen concentration (Table 3) further suggest that *Euryarchaeota* thrive better in colder and recently ventilated waters of the

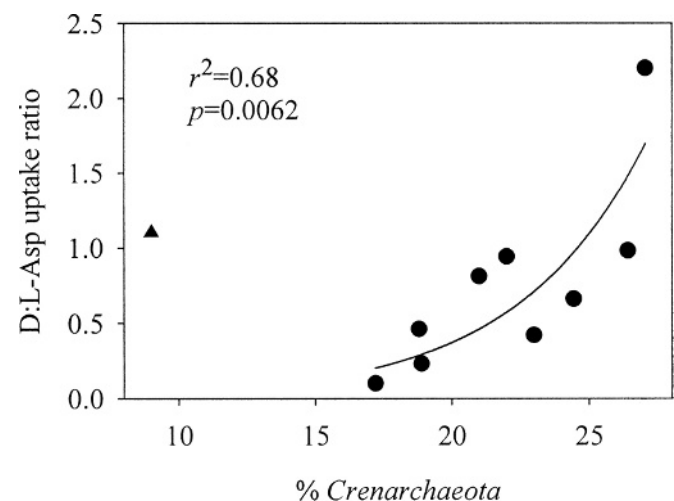


Fig. 7. Relationship between the percentage of *Crenarchaeota* (as % of DAPI-stained cells) and the D:L-Asp uptake ratio. The data point from NEADW (black triangle) has been excluded because the number of samples for *Crenarchaeota* abundance was too low compared with the number of samples for D:L-Asp uptake ratio (see Table 2).

North Atlantic, such as the LSW, than in older water masses.

The generally higher contribution of *Euryarchaeota* to the total prokaryotic community reported here than in previous studies (Karner et al. 2001; Church et al. 2003) might be partially also due to the improved permeabilization procedure of the archaeal cell wall that we applied (see Teira et al. 2004, 2006; Herndl et al. 2005). We used exactly the same procedure for processing all the samples; thus, the observed differences in euryarchaeotal abundance appear to reflect differences in the biogeographic distribution of *Euryarchaeota* in the deep water masses of the North Atlantic. Moreover, cloning and sequencing of selected samples have revealed prokaryotes specific for distinct water masses (Arrieta et al. pers. comm.).

The relative abundance of *Crenarchaeota* was also significantly higher in the western basin, increasing from the SSL toward the deeper water masses (Table 2). The relative abundance of *Crenarchaeota* was also positively correlated with oxygen concentration and was correlated inversely with salinity (Table 3), the latter reflecting the increasing contribution of *Crenarchaeota* to total picoplankton with depth (Table 2). Overall, the contribution of *Crenarchaeota* to the total prokaryotic community was similar to that previously found in the Pacific (Karner et al. 2001) but higher than in the Antarctic Circumpolar Deep Waters (Church et al. 2003; Herndl et al. 2005), which are a mixture of cold oxygen-poor waters from all the main oceans.

#### *Linking prokaryotic community structure and function—*

The notion of the ubiquitous occurrence of Archaea in the marine pelagic environment is relatively recent (DeLong et al. 1994), and only one single strain of a nonthermophilic marine archaeon has been isolated thus far (Könneke et al. 2005). Thus, the factors controlling the distribution of the two major archaeal groups, *Crenarchaeota* and *Euryarchaeota*, in the oxygenated pelagic realm of the global ocean remain largely enigmatic. Very recently, *Crenarchaeota*, including the only isolated nonthermophilic archaeon (*Nitrosopumilus maritimus* gen. et sp. nov.; Könneke et al. 2005) was found to be an ammonia oxidizer, as revealed by the presence of the *amoA* gene (Hallam et al. 2006).

Relating the distribution of specific prokaryotic groups to physical and chemical variables in conjunction with concurrently performed bulk prokaryotic activity measurements (utilization of different substrates, respiration, growth efficiency, growth rate, etc.) can provide valuable clues about the potential role of a specific group in distinct water masses. An important issue to be considered is the fact that all our activity measurements were made under surface-pressure conditions. Decompression of the samples retrieved from greater depth prior to incubation might stimulate or inhibit prokaryotic activity. There is experimental support for both possibilities (Jannasch and Wirsén 1982; Tamburini et al. 2003). Herndl et al. (2005) suggested the possibility of differential sensitivity to pressure changes between Archaea and Bacteria due to the differences in the membrane composition between both groups.

In the present study, we determined the prokaryotic community composition and activity (leucine incorporation and D:L-Asp uptake ratio) in relation to physical and chemical characteristics of the major water masses in order to link the thermohaline ocean circulation to the dynamics in the transformation processes of DOM by the prokaryotic community. Hansell and Carlson (1998) and Hansell (2002) showed that the deep water DOC concentrations in the North Atlantic decline from the Greenland Sea ( $\approx 48 \mu\text{mol L}^{-1}$ ) to  $40^\circ\text{N}$  ( $\approx 44 \mu\text{mol L}^{-1}$ ) in the deep Pacific as a consequence of remineralization and mixing as deep ocean circulation progresses. These authors raised the question on the nature of marine prokaryotes catabolizing recalcitrant DOC at such low rates.

Different water masses were sampled in the western and eastern basin. The variability in prokaryotic distribution and activity did not follow a simple depth- or latitude-related trend (Fig. 4) as previously reported (Dufour and Torr  ton 1996; Nagata et al. 2000) but was more closely related to the different water masses. Thus, we suggest that the distribution of prokaryotes in the deep ocean is not exclusively controlled by the vertical POM (particulate organic matter) flux. Similarly, Hansell and Ducklow (2003) found that POC (particulate organic carbon) export alone does not explain the large variability in bacterial production observed in the mesopelagic realm of several oceanic regions.

As the NADW flows southward and ages, the oxygen concentration decreases, and the inorganic nutrient concentrations increase due to remineralization activity (Figs. 2, 3). This water mass aging of the NADW was more apparent in the eastern than in the western basin. Accordingly, the biological variables showed more latitude-related trends in the NADW in the eastern North Atlantic basin than in the western North Atlantic basin. The prokaryotic activity, the proportion of active cells (estimated as the proportion of prokaryotic cells with enough ribosomes to be detectable by CARD-FISH; see Herndl et al. 2005), and the relative abundance of Archaea were significantly lower in the eastern than the western basin (Fig. 4; Table 2). Prokaryotic turnover rate was significantly lower in the eastern basin as well (Reinthal et al. in press). Therefore, water mass aging appears to be accompanied by structural and functional changes in the prokaryotic community, likely reflecting changes in DOM quality and quantity. Particularly, LSW sampled in the eastern basin showed lower oxygen concentrations (Table 1) than LSW in the western basin, indicating that LSW in the eastern basin is older than in the western basin. Significantly lower prokaryotic activity was measured in this older LSW of the eastern basin, coinciding with a lower euryarchaeotal contribution to picoplankton abundance. Similarly, NEADW, which is older than NADW in the western basin (Moore 2004), showed lower prokaryotic activity (Table 2) and lower relative abundance of Archaea.

The increase in the bulk D:L-Asp uptake ratio with depth has been suggested to be related to a decrease in the supply of L-amino acids with depth (P  rez et al. 2003) due to the preferential uptake of L-amino acids over D-amino acids (J  rgensen et al. 2003). Thus, one would expect an

Table 5. Spearman rank correlation for the oxygen minimum layer of the relative abundance (% of DAPI-stained cells) of Bacteria (Bact), *Crenarchaeota* (Cren), and *Euryarchaeota* (Eury) with ammonia, nitrite, nitrate, leucine uptake (Leu), D- and L-aspartic acid (Asp) uptake, and D:L-Asp uptake ratio (D:L-Asp).

n=16	Ammonia	Nitrite	Nitrate	D-Asp	L-Asp	D:L-Asp	Leu
Bact	0.049	-0.046	-0.182	-0.613*	-0.552*	0.371	-0.445
Cren	0.368	0.603*	-0.045	0.574*	0.530	-0.319	0.588*
Eury	0.349	0.423	0.027	0.297	-0.097	0.444	0.482

\*  $p < 0.05$ .

increase in the D:L-Asp uptake ratio as water masses age. The increasing trend in the D:L-Asp uptake ratio with the age of the water masses is clearly detectable in both the western and the eastern basins. The relatively young source waters of the NADW, the ISOW, DSOW, and the LSW all exhibit significantly lower D:L-Asp uptake ratios than the NADW in both basins (Table 2). When grouping data according to the different water masses, the mean D:L-Asp uptake ratio was positively correlated with relative crenarchaeotal abundance (Fig. 7) but not with leucine incorporation (data not shown). The relative abundance of *Crenarchaeota* explained about 70% of the observed variability in the D:L-Asp uptake ratio. Additional experiments in the western basin using microautoradiography with D- and L-Asp and CARD-FISH showed that *Crenarchaeota* were able to utilize D-Asp as efficiently as L-Asp, whereas Bacteria preferentially used L-Asp (Teira et al. 2006). The results presented here further support the notion of differential utilization of enantiomeric amino acids by the major prokaryotic groups. The slightly lower D:L-Asp uptake ratios in the eastern as compared to the western basin (Table 2) might be due to the lower crenarchaeotal abundance in the water masses of the eastern basin, and, moreover, might reflect subtle differences in the DOM pool of the respective deep water masses in the eastern and western basin. Since less than 20% of the deep water DOM is characterizable on a molecular level, it is impossible to detect such subtle differences in the composition of the DOM (Lee 2004).

Crenarchaeotal and euryarchaeotal abundance was only weakly related to physical and chemical variables (Table 3). Only *Crenarchaeota* exhibited a positive correlation with nitrite concentrations, suggesting a possible involvement of at least some members of this prokaryotic group in nitrogen cycling, possibly as ammonia oxidizers. Several studies have already proposed a connection between planktonic Archaea and the marine nitrogen cycle as denitrifiers or nitrifiers (Murray et al. 1999; Sinninghe Damsté et al. 2002; Wells and Deming 2003). Recently, Könneke et al. (2005) isolated an ammonia oxidizing member of the *Crenarchaeota* from a tropical aquarium. Given that higher ammonia and nitrite oxidation rates are expected to occur in the oxygen minimum layer (Ward 2000), we additionally conducted a correlation analysis of the relative abundance of Bacteria, *Cren*-, and *Euryarchaeota* with ammonia, nitrite, and nitrate concentrations and leucine incorporation, D- and L-Asp uptake, and D:L-Asp uptake ratio in the oxygen minimum layer (Table 5). The abundance of *Crenarchaeota* was related to nitrite concen-

trations, explaining 36% of the variability of crenarchaeotal abundance in this water mass. Moreover, only *Crenarchaeota* were positively related to D-Asp and leucine incorporation, further indicating the potential importance of *Crenarchaeota* in the nitrogen cycling in the oxygen minimum layer. A previous study reported highest concentrations of crenarchaeol, a *Crenarchaeota*-specific membrane lipid near the top of the oxygen minimum zone in the Arabian Sea (Sinninghe Damsté et al. 2002). The potential importance of marine *Crenarchaeota* in the global carbon and nitrogen cycles has also been suggested by Könneke et al. (2005) and Hallam et al. (2006).

In summary, we have shown that the distribution of the major prokaryotic groups is closely linked to the major water masses of the thermohaline circulation system. Bacteria contribute, on average, around 30% to the total picoplankton abundance in the different water masses of the North Atlantic. *Euryarchaeota* are most abundant in cold, recently formed, deep water masses with low salinity (<34.9) and high oxygen concentration (such as LSW and DSOW); however, they are otherwise relatively uniformly distributed throughout the North Atlantic water column. *Crenarchaeota* exhibit their highest abundance in the O<sub>2</sub> minimum layer and correlate with nitrite concentrations, suggesting that members of the *Crenarchaeota* are involved in nitrification processes in the O<sub>2</sub> minimum layer.

## References

- AKEN, H. M. v. 2000a. The hydrography of the mid-latitude northeast Atlantic Ocean: I. The deep water masses. *Deep-Sea Res. I* **47**: 757–788.
- . 2000b. The hydrography of the mid-latitude northeast Atlantic Ocean: II. The intermediate water masses. *Deep-Sea Res. I* **47**: 789–824.
- AMANN, R. I., W. LUDWIG, AND K. H. SCHLEIFER. 1995. Phylogenetic identification and in situ detection of individual microbial cells without cultivation. *Microbiol. Rev.* **59**: 143–169.
- BANO, N., S. RUFFIN, B. RANSOM, AND J. T. HOLLIBAUGH. 2004. Phylogenetic composition of Arctic Ocean archaeal assemblages and comparison with Antarctic assemblages. *App. Environ. Microbiol.* **70**: 781–789.
- BAUER, J. E., P. M. WILLIAMS, AND E. R. M. DRUFFEL. 1992. <sup>14</sup>C activity of dissolved organic carbon fractions in the north-central Pacific and Sargasso Sea. *Nature* **357**: 667–670.
- BENNER, R., J. D. PAKULSKI, M. MCCARTHY, J. I. HEDGES, AND P. G. HATCHER. 1992. Bulk chemical characteristics of dissolved organic matter in the ocean. *Science* **255**: 1561–1564.
- BROECKER, W. S. 1997. Thermohaline circulation, the Achilles heel of our climate system: Will man-made CO<sub>2</sub> upset the current balance? *Science* **278**: 1582–1588.

- CHURCH, M. J., E. F. DELONG, H. W. DUCKLOW, M. B. KARNER, C. M. PRESTON, AND D. M. KARL. 2003. Abundance and distribution of planktonic Archaea and Bacteria in the waters west of the Antarctic Peninsula. *Limnol. Oceanogr.* **48**: 1893–1902.
- DAIMS, H., A. BRÜHL, R. AMANN, K.-H. SCHLEIFER, AND M. WAGNER. 1999. The domain-specific probe EUB338 is insufficient for the detection of all bacteria: Development and evaluation of a more comprehensive probe set. *System. Appl. Microbiol.* **22**: 434–444.
- DELONG, E. F., K. Y. WU, B. B. PRÉZELIN, AND R. V. M. JOVINE. 1994. High abundance of Archaea in Antarctic marine picoplankton. *Nature* **371**: 695–697.
- DUFOUR, P. H., AND J.-P. TORRÉTON. 1996. Bottom-up and top-down control of bacterioplankton from eutrophic to oligotrophic sites in the tropical northeastern Atlantic Ocean. *Deep-Sea Res. I* **43**: 1305–1320.
- FINLAY, B. J. 2002. Global dispersal of free-living microbial eukaryote species. *Science* **296**: 1061–1063.
- GIOVANNONI, S., AND M. RAPPÉ. 2000. Evolution, diversity, and molecular ecology of marine prokaryotes, p. 47–84. *In* D. L. Kirchman [ed.], *Microbial ecology of the oceans*. Wiley-Liss.
- HALLAM, S. J., T. J. MINCER, C. SCHLEPER, C. M. PRESTON, K. ROBERTS, P. M. RICHARDSON, AND E. F. DELONG. 2006. Pathways of carbon assimilation and ammonia oxidation suggested by environmental genomic analyses of marine *Crenarchaeota*. *PLoS. Biol.* **4**: e95.
- HANSELL, D. A. 2002. DOC in the global ocean carbon cycle, p. 685–715. *In* Hansell, D. A. and C. A. Carlson [eds.], *Biogeochemistry of marine dissolved organics matter*. Academic Press.
- , AND C. A. CARLSON. 1998. Deep-ocean gradients of dissolved organic carbon. *Nature* **395**: 443–453.
- , AND H. W. DUCKLOW. 2003. Bacterioplankton distribution and production in the bathypelagic ocean: Directly coupled to particulate organic carbon export? *Limnol. Oceanogr.* **48**: 150–156.
- HELDER, W., AND R. DE VRIES. 1979. An automatic phenol-hypochlorite method for the detection of ammonia in sea- and brackish waters. *J. Sea Res.* **13**: 154–160.
- HERNDL, G. J., T. REINTHALER, E. TEIRA, H. VAN AKEN, C. VETH, A. PERNTHALER, AND J. PERNTHALER. 2005. Contribution of Archaea to total prokaryotic production in the deep Atlantic Ocean. *Appl. Environ. Microbiol.* **71**: 2303–2309.
- JANNASCH, H. J., AND C. O. WIRSEN. 1982. Microbial activities in undecompressed microbial populations from the deep seawater samples. *Appl. Environ. Microbiol.* **43**: 1116–1124.
- JØRGENSEN, N. O. G., R. STEPANOUKAS, A.-G. U. PEDERSEN, M. HANSEN, AND O. NYBROE. 2003. Occurrence and degradation of peptidoglycan in aquatic environments. *FEMS Microbiol. Ecol.* **46**: 269–280.
- KARNER, M. B., E. F. DELONG, AND D. M. KARL. 2001. Archaeal dominance in the mesopelagic zone of the Pacific Ocean. *Nature* **409**: 507–510.
- KÖNNEKE, M., A. E. BERNHARD, J. R. DE LA TORRE, C. B. WALKER, J. B. WATERBURY, AND D. A. STAHL. 2005. Isolation of an autotrophic ammonia-oxidizing marine archaeon. *Nature* **437**: 543–546.
- LEBARON, P., N. PARTHUISOT, AND P. CATALA. 1998. Comparison of blue nucleic acid dyes for flow cytometric enumeration of bacteria in aquatic systems. *Appl. Environ. Microbiol.* **64**: 1725–1730.
- LEE, C. 2004. Transformations in the “twilight zone” and beyond. *Mar. Chem.* **92**: 87–90.
- LÓPEZ-GARCÍA, P., A. LÓPEZ-LÓPEZ, D. MOREIRA, AND F. RODRÍGUEZ-VALERA. 2001. Diversity of free-living prokaryotes from a deep-sea site at the Antarctic Polar Front. *FEMS Microbiol. Ecol.* **36**: 193–202.
- MASSANA, R., E. F. DELONG, AND C. PEDRÓS-ALIÓ. 2000. A few cosmopolitan phylotypes dominate planktonic archaeal assemblages in widely different oceanic provinces. *Appl. Environ. Microbiol.* **66**: 1777–1787.
- , L. T. TAYLOR, A. E. MURRAY, K. Y. WU, W. H. JEFFREY, AND E. F. DELONG. 1998. Vertical distribution and temporal variation of marine planktonic archaea in the Gerlache Strait, Antarctica, during early spring. *Limnol. Oceanogr.* **43**: 607–617.
- MCCARTNEY, M., K. DONOHUE, R. CURRY, C. MAURITZEN, AND S. BACON. 1998. Did the overflow from the Nordic Seas intensify in 1996–1997? *International WOCE Newsletter* **31**: 3–7.
- MOORE, R. M. 2004. Dichloromethane in North Atlantic waters. *J. Geophys. Res.* **109**: C09004.
- MURPHY, J., AND J. P. RILEY. 1962. A modified single solution method for the determination of phosphate in natural waters. *Anal. Chim. Acta* **27**: 31–36.
- MURRAY, A. E., A. BLAKIS, R. MASSANA, S. STRAWZEWSKI, U. PASSOW, A. ALLDREDGE, AND E. F. DELONG. 1999. A time series assessment of planktonic archaeal variability in the Santa Barbara channel. *Aquat. Microb. Ecol.* **20**: 129–145.
- NAGATA, T., H. FUKUDA, R. FUKUDA, AND I. KOIKE. 2000. Bacterioplankton distribution and production in deep Pacific waters: Large-scale geographic variations and possible coupling with sinking particle fluxes. *Limnol. Oceanogr.* **45**: 426–435.
- OUPERNEY, C. C., AND J. A. FUHRMAN. 2000. Marine planktonic Archaea take up amino acids. *Appl. Environ. Microbiol.* **66**: 4829–4833.
- PARSONS, T., Y. MAITA, AND Y. LALLI. 1984. *A manual of chemical and biological methods for seawater analysis*. Pergamon Press.
- PATCHING, J. W., AND D. EARDLY. 1997. Bacterial biomass and activity in the deep waters of the eastern Atlantic—evidence of a barophilic community. *Deep-Sea Res. I* **44**: 1655–1670.
- PEDRÓS-ALIÓ, C. 1993. Diversity of bacterioplankton. *TREE* **8**: 86–90.
- PÉREZ, M. T., C. PAUSZ, AND G. J. HERNDL. 2003. Major shift in bacterioplankton utilization of enantiomeric amino acids between surface waters and the ocean’s interior. *Limnol. Oceanogr.* **48**: 755–763.
- REINTHALER, T., H. VAN AKEN, C. VETH, P. LEBARON, J. ARISTEGUI, C. ROBINSON, P. J. LE. B. WILLIAMS, AND G. J. HERNDL. *In press*. Prokaryotic respiration and production in the meso- and bathypelagic realm of the eastern and western North Atlantic basin. *Limnol. Oceanogr.*
- RHEIN, M., J. FISCHER, W. M. SMETHIE, D. SMYTHE-WRIGHT, R. F. WEISS, C. MERTENS, D.-H. MIN, U. FLEISCHMANN, AND A. PUTZKA. 2002. Labrador Sea Water: Pathways, CFC inventory and formation rates. *J. Phys. Oceanogr.* **32**: 648–665.
- SINNINGHE DAMSTÉ, J. S., W. I. C. RIJSTRA, E. C. HOPMANS, F. G. PRAHL, S. G. WAKEHAM, AND S. SCHOUTEN. 2002. Distribution of membrane lipids of planktonic *Crenarchaeota* in the Arabian Sea. *Appl. Environ. Microbiol.* **68**: 2997–3002.
- SMETHIE, W. M., R. A. FINE, A. PUTZKA, AND E. P. JONES. 2000. Tracing the flow of North Atlantic Deep Water using chlorofluorocarbons. *J. Geophys. Res.* **105**: 14297–14323.
- TAMBURINI, C., J. GARCIN, AND A. BIANCHI. 2003. Role of deep-sea bacteria in organic matter mineralization and adaptation to hydrostatic pressure conditions in the NW Mediterranean Sea. *Aquat. Microb. Ecol.* **32**: 209–218.

- TEIRA, E., T. REINTHALER, A. PERNTHALER, J. PERNTHALER, AND G. J. HERNDL. 2004. Combining catalyzed reporter deposition-fluorescence in situ hybridization and microautoradiography to detect substrate utilization by Bacteria and Archaea in the deep ocean. *Appl. Environ. Microbiol.* **70**: 4411–4414.
- , H. VAN AKEN, C. VETH, AND G. J. HERNDL. 2006. Archaeal uptake of enantiomeric amino acids in meso- and bathypelagic waters of the North Atlantic. *Limnol. Oceanogr.* **51**: 60–69.
- WARD, B. B. 2000. Nitrification and the marine nitrogen cycle, p. 427–453. *In* D. L. Kirchman [ed.], *Microbial ecology of the oceans*. Wiley-Liss.
- WELLS, L. E., AND J. W. DEMING. 2003. Abundance of Bacteria, the Cytophaga-Flavobacterium cluster and Archaea in cold oligotrophic waters and nepheloid layers of the Northwest Passage, Canadian Archipelago. *Aquat. Microb. Ecol.* **31**: 19–31.
- WUCHTER, C., S. SCHOUTEN, H. T. S. BOSCHKER, AND J. S. S. DAMSTÉ. 2003. Bicarbonate uptake by marine Crenarchaeota. *FEMS Microb. Lett.* **219**: 203–207.

*Received: 22 November 2005*

*Accepted: 27 April 2006*

*Amended: 16 May 2006*